Quantification of Ligand-Regulated Nuclear Receptor Corepressor and Coactivator Binding, Key Interactions Determining Ligand Potency and Efficacy for the Thyroid Hormone Receptor[†]

M. Jeyakumar,[‡] Paul Webb,[§] John D. Baxter,[§] Thomas S. Scanlan,[||] and John A. Katzenellenbogen*[,‡]

Department of Chemistry, University of Illinois, Urbana, Illinois 61801, Diabetes Center and Metabolic Research Unit, University of California, San Francisco, California 94143, and Department of Physiology and Pharmacology, Oregon Health and Science University, Portland, Oregon 97239

Received March 6, 2008; Revised Manuscript Received May 9, 2008

ABSTRACT: The potency and efficacy of ligands for nuclear receptors (NR) result both from the affinity of the ligand for the receptor and from the affinity that various coregulatory proteins have for ligand−receptor complexes; the latter interaction, however, is rarely quantified. To understand the molecular basis for ligand potency and efficacy, we developed dual time-resolved fluorescence resonance energy transfer (tr-FRET) assays and quantified binding of both ligand and coactivator or corepressor to the thyroid hormone receptor (TR). Promoter-bound TR exerts dual transcriptional regulatory functions, recruiting corepressor proteins and repressing transcription in the absence of thyroid hormones (THs) and shedding corepressors in favor of coactivators upon binding agonists, activating transcription. Our tr-FRET assays involve a TRE sequence labeled with terbium (fluorescence donor), TRβ·RXRα heterodimer, and fluorescein-labeled NR interaction domains of coactivator SRC3 or corepressor NCoR (fluorescence acceptors). Through coregulator titrations, we could determine the affinity of SRC3 or NCoR for TRE-bound TR·RXR heterodimers, unliganded or saturated with different THs. Alternatively, through ligand titrations, we could determine the relative potencies of different THs. The order of TR agonist potencies is as follows: GC-1 $\sim$ T_3 $\sim$ TRIAC $\sim$ T_4 $\gg$ rT_3 (for both coactivator recruitment and corepressor dissociation); the affinities of SRC3 binding to TR−ligand complexes followed a similar trend. This highlights the fact that the low activity of rT_3 is derived both from its low affinity for TR and from the low affinity of SRC for the TR−rT_3 complex. The TR antagonist NH-3 failed to induce SRC3 recruitment but did effect NCoR dissociation. These assays provide quantitative information about the affinity of two key interactions that are determinants of NR ligand potency and efficacy.

Our evolving understanding of the processes by which nuclear receptors (NRs)[1] regulate gene transcription has revealed an increasing number of protein partners with which a receptor interacts to alter chromatin architecture and nucleosome structure, and to regulate the activity of RNA polymerase II. The best-characterized proximal protein partners of the NRs are the p160 coactivators, exemplified by steroid receptor coactivator 3 (SRC3), and corepressors, exemplified by the nuclear receptor corepressor (NCoR). Both of these proteins interact with the NRs through specific nuclear receptor interaction domains (NRIDs) in a ligand-dependent manner, with the corepressor binding to unliganded or antagonist-liganded NR states that repress transcription and the coactivator binding to agonist-liganded NR states that activate transcription (*1, 2*).

While in general, the potency of a NR ligand is related to the affinity with which it binds to its cognate receptor, potency and affinity do not always track in parallel; in particular, as the structure of a ligand is changed, it is sometimes observed that potency decreases faster than binding affinity. This more rapid decrease in potency could arise at the level of the receptor−coactivator interaction if, for example, a coactivator bound more weakly to a receptor−low-affinity ligand complex than to a receptor−high-affinity ligand complex, even if the receptor was fully saturated with ligands in both cases. Thus, ligand potency would be determined by a combination of two interactions, (i) the affinity of the ligand for binding to the receptor and (ii) the affinity of the coactivator for binding to the ligand−receptor complex.

To study these two key interactions that are thought to underlie the potency of NR ligands directly, we have

[†] This work was supported by grants from the National Institutes of Health (PHS R37 DK15556, P01 AG 24387A4-Project-4 to J.A.K., PHS R01 DK64148 to J.D.B., and PHS R01 DK52798 to T.S.S.).

* To whom correspondence should be addressed: Department of Chemistry, University of Illinois, 600 S. Mathews Ave., Urbana, IL 61801. Phone: (217) 333-6310. Fax: (217) 333-7325. E-mail: jkatzene@uiuc.edu.

[‡] University of Illinois.

[§] University of California.

[||] Oregon Health and Science University.

[1] Abbreviations: DMSO, dimethyl sulfoxide; DR+4, direct repeat spaced by four nucleotides; Fl, fluorescein; NCoR, nuclear receptor corepressor; NR, nuclear receptor; NRID, nuclear receptor interaction domain; RXR, retinoid X receptor; SA, streptavidin; SRC3, steroid receptor coactivator 3; Tb, terbium; TH, thyroid hormone; tr-FRET, time-resolved fluorescence resonance energy transfer; TR, thyroid hormone receptor; TRE, thyroid hormone response element.

10.1021/bi800393u CCC: $40.75 © 2008 American Chemical Society
Published on Web 06/18/2008

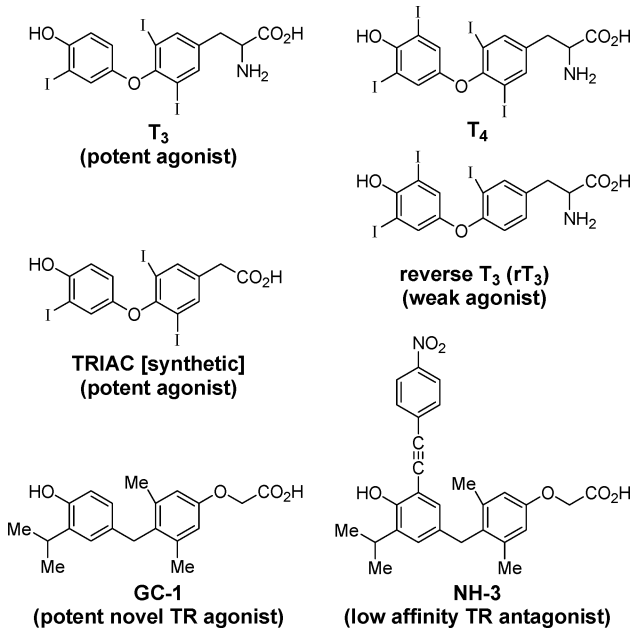

FIGURE 1: Structures of the different ligands used: endogenous thyroid hormones, T_3, T_4, and rT_3; synthetic TRβ-selective agonists, TRIAC and GC-1; and an antagonist, NH-3.

developed dual in vitro, time-resolved fluorescence resonance energy transfer-based assays, using purified components, through which it is possible to examine in a convenient and quantitative manner both ligand-induced association of the SRC3 NRID with a NR and ligand-induced displacement of the NCoR NRID from the same NR. We have used this assay to study these interactions in the context of the thyroid hormone receptor (TR) and its ligands, the thyroid hormones (THs).

The TR−TH system is a particularly good one for this purpose, because the TR remains a promoter bound both in the absence and in the presence of ligands, with unliganded TR recruiting corepressors and repressing gene transcription, and the agonist-liganded TR recruiting coactivators and activating gene transcription (*3*). Furthermore, there are both high- and low-affinity, low-potency TR ligands, both natural (T_3 and T_4 vs rT_3) and synthetic (TRIAC and GC-1), as well as a recently described TR antagonist (NH-3) (Figure 1). The THs play essential roles in mammalian development, growth, and homeostasis (*4*), and the human thyroid gland produces T_4, the major TH, and relatively smaller amounts of T_3 and rT_3. T_3 binds to the TR with the highest affinity and rT_3 with the lowest (*5–8*). Thus, T_4 is the major thyroid hormone, while T_3 is the most potent one.

Our tr-FRET assays recapitulate many of the molecular elements involved in TH regulation of transcription in cells: a direct repeat [DR+4 thyroid hormone response element (TRE) sequence from a known TH-regulated gene (labeled with terbium-strepavidin, the fluorescence donor)], TRβ with its usual heterodimer partner RXRα (*9–12*), and nuclear receptor interaction domains of the coactivator SRC3 (*13, 14*) or the corepressor NCoR (labeled with fluorescein as the fluorescence acceptor) (*15, 16*). The tr-FRET assays can be set up to measure either the affinity with which the coactivator or the corepressor binds to TR·RXR while it is TRE-bound (coregulator titration mode) or the potency and efficacy with which a ligand dissociates NCoR or recruits SRC3 to the TRE-bound receptors (ligand titration mode).

With these assays, we have found both expected and unexpected trends in the relationship between the potencies with which ligands bind to TR and the affinities with which coactivators bind to ligand−TR complexes. We have characterized the basis for the low potency of rT_3 and explored how T_4 differs from T_3 and TRIAC in these interactions, and we have characterized the distinctly different coregulator recruitment patterns of TR agonists and antagonists. This convenient and versatile assay provides quantitative information about the affinity of two key interactions that are determinants of ligand potency and efficacy and should prove to be useful in investigations of both ligand discovery and molecular pharmacology with other nuclear receptor systems.

EXPERIMENTAL PROCEDURES

Reagents. T_4 (3,5,3′,5′-tetraiodo-L-thyronine), T_3 (3,5,3′-triiodo-L-thyronine), TRIAC (triiodoacetic acid), rT_3 (3,3′,5′-triiodo-L-thyronine), 2-thioglycerol, and Sephadex G-25 (medium) were purchased from Sigma (St. Louis, MO). Calf thymus DNA was from Calbiochem. [^{125}I]T_4 (116 Ci/mmol) and [^{125}I]T_3 (97 Ci/mmol) were obtained from PerkinElmer. GC-1 [3,5-dimethyl-4-(4′-hydroxy-3′-isopropylbenzyl)phenoxylacetic acid] and NH-3 ({4-[4-hydroxy-3-isopropyl-5-(4-nitrophenylethynyl)benzyl]-3,5-dimethylphenoxy}acetic acid) have been described previously (*17, 18*). The thiol reactive flurophores, 5-iodoacetamidofluorescein and terbium-labeled streptavidin, were obtained from Molecular Probes/Invitrogen (Eugene, CA) and Invitrogen (Carlsbad, CA), respectively. A 48 bp DNA sequence containing a single-copy DR+4 TRE (5′/5Bio/GAACAGATCTCCTTGGCTCTG-GAGGTCACAGGAGGTCAGCGGATCCAT; core TRE underlined) was derived from the rat α-myosin heavy chain promoter and was synthesized by Integrated DNA Technologies (Coralville, IA) (*19*). Biotin was covalently attached to 5′ end of the sense strand. The core DR+4 sequence, AGGTGACAGGAGGACA, from the natural promoter was changed to the consensus DR+4 sequence AGGTCACAG-GAGGTCA.

Plasmids and Protein Expression. The bacterial expression plasmids encoding six-His fusion proteins of hTRβ (amino acids 82−456 containing both the DNA and ligand binding domains), hRXRα (full length), and a GST-tagged NCoRC′ encoding the NRID fragment mNCoR (residues 2057−2453) were kindly provided by M. K. Bagchi, and their functional properties have been described previously (*20–22*). The *Nde*I−*Bam*HI fragment of NCoRC′ from the GST−NCoRC′ vector was excised and cloned into the NdeI and BamHI sites of the pET15b vector and expressed as a six-His fusion protein. Expression of the NRID fragment of the hSRC3 protein (residues 627−829) has been previously described (*23*). The NRID fragments of SRC3 and NCoR were fluorescently labeled with 5-iodoacetamidofluorescein according to our published procedure (*23, 24*).

HPLC Analysis of TR Ligands. T_4, T_3, and rT_3 were tested for their purity in an analytical C18 reversed phase column (Waters-Symmetry, 5 μm, 4.6 mm × 150 mm) using a gradient from 20 to 45% acetonitrile in water. While T_3 was found to be pure, the T_4 stock was found to contain 0.08% T_3, and rT_3 was found to contain 0.09% T_4. Peak fractions of T_4 and rT_3 devoid of contaminants were collected, verified for purity on the same column, and used in our experiments.

Coregulator (SRC3 or NCoR) Titration Assays. Fluorescein-labeled SRC3 or NCoR fragment was serially diluted at 1.5 times the required final concentration in 1.5 mL amber microfuge tubes in buffer A [50 mM Tris (pH 8) containing 10% glycerol, 0.05% Nonidet P-40, 50 mM KCl, 2 mM β-mercaptoethanol, and 0.3 mg/mL ovalbumin], and 10 μL aliquots of each dilution were added to the wells of a 96-well dark microplate (Molecular Devices, Sunnyvale, CA). TR ligands were dissolved at a concentration of 20 mM in 0.1 M NaOH (T_3, TRIAC, T_4, and rT_3) or 5 mM in DMSO (T_3, GC-1, and NH-3). Ligands in NaOH or DMSO were further diluted in buffer B [20 mM Tris (pH 8) and 100 mM NaCl] or buffer B containing 6% DMSO. A 3× premixture of SA-Tb, TRE, TR, RXR, and various TR ligands or an equivalent volume of the solvents was prepared and then added to each well in a volume of 5 μL for final assay concentrations of 2.5 nM (SA-Tb), 10 nM (TRE), 15 nM (TR and RXR each), and 3 μM (ligands). The total assay volume was 15 μL.

Each assay was conducted with corresponding negative control wells that contained all the components with appropriately diluted solvents, but without the biotinylated TRE, which was used to correct for diffusion-enhanced FRET. The plates were gently mixed, protected from light, and incubated for 1 h at room temperature before measurement for tr-FRET. Coregulator titrations performed in the presence of 10, 15, and 25 nM TR·RXR indicated that 15 nM TR·RXR was the lowest receptor concentration to yield an optimal assay sensitivity and assay window. Incubation of assay plates for different times indicated that the reaction reached equilibrium by 1 h and the tr-FRET signal remained unchanged for up to 24 h (data not shown).

Ligand Titration Assays. The following 3× reaction components were made: ligand or solvent dilutions in buffer B or buffer B with 6% DMSO, fluorescein-labeled coregulators in buffer A, and a premixture of SA-Tb, TR·RXR with (test) or without (control) biotinylated TRE in buffer A. Aliquots (5 μL) of different ligand dilutions and the SA-Tb−DNA receptor heterodimer premixture were added first, followed by the addition of 5 μL of fluorescein-labeled SRC3 or NCoR. The final assay concentrations for SA-Tb, TRE, TR·RXR, and fluorescein-labeled SRC3 or NCoR in each well were 2.5, 10, 15, and 125 or 24 nM, respectively, in the presence of the indicated ligand concentrations. Diffusion-enhanced background fluorescence was measured as described in the previous experiment. The plates were mixed gently and assessed for tr-FRET after incubation for 1 h at room temperature in the dark.

Ligand Dissociation Kinetic Assays. T_4 and T_3 dissociation experiments were carried out essentially as previously described, except that ligand dissociations were carried out at 25 °C instead of 4 °C (*6*). Briefly, 3.0 nM TRβ alone or in complex with equimolar RXR or RXR with DR+4 TRE was allowed to bind 25 nM [^{125}I]T_4 or [^{125}I]T_3 in buffer (pH 8.0) containing 20 mM $KHPO_4$, 150 mM NaCl, 0.5 mM EDTA, 1.0 mM $MgCl_2$, 1 mM 2-thioglycerol, and 500 μg/mL calf thymus histones (700 μL reaction volume) until the reaction reached equilibrium (12 h at 4 °C). In some assays, we used a saturating concentration (100 nM) of unlabeled SRC3 protein along with the other combinations described above. Following incubation, tubes were warmed in a 25 °C water bath for 30 min, and a 50 μL aliquot was applied to a Sephadex G-25 column (2 mL) before and at different time points after the addition of excess (2.0 μM) unlabeled T_4 or T_3. Receptor-bound radioactivity was collected and counted in a γ-counter.

Inhibition of T_3 and GC-1-Dependent SRC3 Recruitment by NH-3. Five microliters of serially diluted NH-3 (as 4×) in buffer B containing 4% DMSO was individually mixed with 5 μL of either T_3 or GC-1 (either at 120 nM) in buffer B containing 4% DMSO. Five microliters each of 500 nM fluorescein-labeled SRC3 and 4× SA-Tb and TR·RXR with (test) or without (control) biotinylated TRE was then added to the ligand mixture. The final concentrations of T_3 or GC-1 and SRC3 were 30 and 125 nM and of SA-Tb, TRE, and TR·RXR 2.5, 10, and 15 nM, respectively.

While the presence of 2% DMSO in assays had no significant effect on the EC_{50} values for SRC3 recruitment, we observed a modest decrease in the affinity of NCoR for the unliganded TR, with a concomitant decrease in IC_{50} values in NCoR dissociation assays in the presence of DMSO (compare Figures 5B and 6 with panels C and D of Figure 8). However, in NCoR dissociation assays performed in the presence and absence of DMSO (2%), the relative potencies of different TR ligands remained essentially unchanged (data not shown).

tr-FRET Measurements. tr-FRET was assessed on a Wallac Victor II plate reading fluorometer (Molecular Devices, Sunnyvale, CA) as previously described (*25*).

Statistical Analysis. Assays were performed in replicates, and each point in the binding curves represents the mean ± standard deviation of three independent experiments. The Z' factor was calculated from six replicates of specific tr-FRET values corresponding to the maximal response values (saturation points) and their respective negative control values for coregulator saturation assays [at 0.5 and 1 μM SRC3 in the presence (positive control) and absence (negative control) of different TR ligands at 3 μM in the coactivator titration assay and at 0.125 and 0.25 μM NCoR in the absence (positive control) and presence (negative control) of 3 μM ligands in the corepressor titration assay], using a previously described method (*26*). The Z' factors were similarly determined for ligand titrations of both SRC3 recruitment and NCoR dissociation using the respective positive and negative control values. The Z' equation is

$$Z' = 1 - [(3\sigma_{c1} + 3\sigma_{c2})/(\mu_{c1} - \mu_{c2})]$$

where σ_{c1} and σ_{c2} are the standard deviations of the positive and negative control values, respectively, and μ_{c1} and μ_{c2} are mean values for the positive and negative controls, respectively. The Z' value of each ligand and of different ligands tested in a given experiment is provided as a range in the respective figure legends.

The dose-dependent NH-3 displacement curve of agonist-induced SRC3 binding was analyzed by the Cheng−Prusoff equation to determine the relative affinities of NH-3 in blocking SRC3−TR interaction in the presence of a 30 nM minimal dose of T_3 or GC-1 (*27*).

RESULTS

Time-Resolved Fluorescence Resonance Energy Transfer (tr-FRET) Assays of TR−Coregulator Interactions. tr-FRET is a convenient, fluorescence-based assay technology for

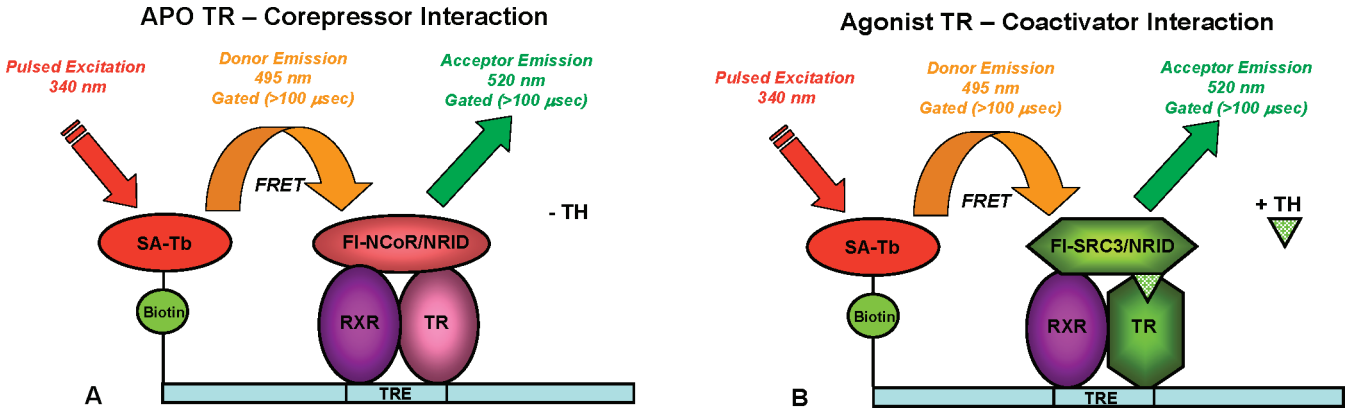

FIGURE 2: Principle of the dual tr-FRET assays. (A) NCoR interacts with the unliganded TR·RXR heterodimer bound to a TRE. A hTRβ (residues 82−456)·hRXRα (full length) heterodimer was assembled onto a terbium-labeled streptavidin-bound biotinylated DR+4 sequence (49 bp derived from the rat myosin heavy chain promoter) and incubated with the fluorescein-labeled NRID fragment of mNCoR (residues 2057−2453). The terbium (donor) was excited at 340 nm, and tr-FRET was assessed after a 100 μs delay at 495 nm for terbium (donor) and 520 nm for fluorescein (acceptor). (B) SRC3 interacts with the liganded TR·RXR heterodimer bound to a TRE. The assay format is essentially the same as that described for panel A, except that the recruitment of the fluorescein-labeled NRID fragment of hSRC3 (residues 627−829) to TRE-bound TR·RXR was assessed in the presence of different TR ligands.

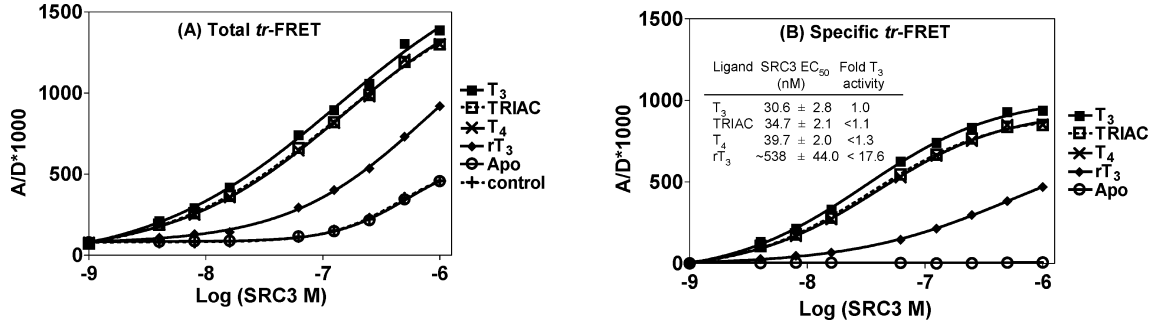

FIGURE 3: Ligands specify affinity of SRC3 for TRE-bound TR·RXR heterodimers (coactivator titration). (A) A fixed amount of TR·RXR heterodimer (15 nM) bound to a biotinylated TRE was incubated with increasing concentrations of fluorescein-labeled SRC3 (NRID fragment) in the absence (apo) and presence of 3 μM T_3, TRIAC, T_4, and rT_3, as described in Experimental Procedures. Control assays containing all the components except the biotinylated DNA were used to correct for diffusion-enhanced FRET. After incubation at room temperature for 1 h, the level of tr-FRET was measured and plotted as the ratio of acceptor to donor × 1000 ($A/D \times 1000$) vs the log of fluorescein-labeled SRC3 concentration. The binding curves obtained for different ligands and the control are shown. (B) The tr-FRET values presented in each of the binding curves in panel A were subtracted from the corresponding diffusion-enhanced FRET values, and the resulting specific FRET units are plotted vs the log SRC3 concentrations. Three independent sets of experiments were performed in replicate, and each assay point in the binding curves represents the mean ± standard deviation of six measurements. Data in panel B were analyzed by nonlinear regression with an equation for the sigmoidal dose response (variable slope) in GraphPad Prism, and the concentrations of fluorescein-labeled SRC3 at 50% (EC_{50}) of maximal binding in the presence of the indicated TR ligands were obtained and are listed in the table as mean EC_{50} values ± the standard deviation of three different experiments. Fold T_3 activity was calculated as the ratio of the respective ligand EC_{50} value to that of T_3. The Z' factor was calculated by using the six replicates of maximally responsive specific tr-FRET values obtained with each ligand and the corresponding value obtained in the absence of ligand (apo) as described in Experimental Procedures. The Z' factor for SRC3 recruitment by each ligand ranged from 0.80 to 0.84.

studying molecular interactions, which can be adapted to a microplate format, that we have used to quantify the ligand-regulated interactions of a corepressor and a coactivator with hTRβ. To determine both the binding affinity and the ligand-dependent displacement of fluorescein-labeled NCoR from, and the recruitment of fluorescein-labeled SRC3 (both as NRID fragments) to, TRE-bound hTRβ·hRXRα heterodimers, we used TR·RXR indirectly labeled with terbium via a biotinylated TRE that is linked to a streptavidin−terbium (SA−Tb) conjugate. Excitation of the Tb chelate at 340 nm results in emission at 495 nm. However, if both TRE-bound TR and coregulator are close to each other, energy from the excited state of the Tb complex can be transferred to the fluorescein acceptor, which emits at 520 nm (Figure 2A,B). By monitoring the degree of FRET as the ratio of acceptor emission intensity (A, at 520 nm) to donor emission intensity (D, at 495 nm), expressed as $A/D \times 1000$, we could follow quantitatively the ligand-dependent association and dissociation of coregulators with the TRE-bound TR.

Determination of SRC3 Binding Affinity for Various TR−Ligand Complexes: Coactivator Titration Assay. A coactivator titration assay is used to measure the affinity of SRC3 for the TRE-bound TR·RXR heterodimer. As shown in Figure 3A, when increasing concentrations of fluorescein-labeled SRC3 NRID were incubated with a fixed amount of DNA-bound TR·RXR (15 nM) and a fixed, saturating concentration of different TR ligands (3 μM, or in the absence of ligand, apo TR), we observed a concentration-dependent and ligand-specific increase in the magnitude of the tr-FRET signal, reflecting the binding of SRC3 to the various TR−ligand complexes. To correct for diffusion-enhanced FRET, background control fluorecence (tr-FRET assessed in the absence of biotinylated DNA) is subtracted from the total tr-FRET values. This shows that specific

binding approaches full saturation at the highest SRC3 concentration for all the ligands tested, except for rT_3 (Figure 3B). The baseline binding in Figure 3B indicated that SRC3 did not bind at all to the unliganded TR·RXR [apo vs control (Figure 3A)]. In preliminary experiments, SRC3 titration was performed at 1.0, 2.0, 3.0, 10.0, and 100 μM for the different ligands. We found that saturable binding of SRC3 to TR was observed at 3 μM T_3, TRIAC, and T_4. With rT_3, SRC3 did not reach a clear saturation plateau even at a concentration of 100 μM, although the level of SRC3 recruitment increased to 85% of that induced by 3 μM TRIAC or T_4 (data not shown). Since we were interested in comparing the coactivator recruitment profiles of the TR exposed to the same concentration of different ligands, a concentration of 3 μM was used for all the ligands.

The concentration of SRC3 that gives 50% binding (EC_{50}), a measure of the apparent affinity of SRC3 for these TR−ligand complexes, was found to be 30.6 ± 2.8, 34.7 ± 2.1, 39.7 ± 2.0, and 538 ± 44 nM for T_3, TRIAC, T_4, and rT_3, respectively (Figure 3B and table). The comparable EC_{50} and maximal binding (B_{max}) values with T_3, TRIAC, and T_4 indicate that these ligands induce conformations in TRβ that have similar affinities for SRC3. By contrast, the 18-fold larger EC_{50} value for rT_3 indicates that this ligand stabilizes a TR conformation with much lower affinity for SRC3 but nevertheless suggests that rT_3 has potential agonistic activity. Earlier results from in vitro GST pull-down assays showed that some TR agonists had the same coactivator binding capacity (*6, 20, 28*); by contrast, our tr-FRET assay provides a direct measurement of both the binding capacity and the binding affinity of SRC3 for these different TR−ligand complexes.

The specificity of these TR−coregulator interactions was verified by confirming a complete loss of tr-FRET signal when the TRE half-site AGGTCA sequence was mutated to TCTCTG. Gel shift assays confirmed the sequence specificity of the TRE interaction and showed that, in the presence of RXR, TR interacted with the DR+4 response element predominantly (>95%) as TR·RXR heterodimers. Ligands had no effect on this interaction (data not shown).

Determination of Ligand Potency for TR−SRC3 Recruitment: Ligand Titration. A ligand titration assay was used to assess the relative potencies of different TR ligands in recruiting SRC3. The concentration of fluorescein-labeled SRC3 used in this ligand titration assay, 125 nM, was selected from the previous experiment (Figure 3B) to provide a near maximum specific tr-FRET signal and a minimum nonspecific signal for most ligands with the concentration of TRE-bound TR·RXR heterodimers required to obtain a good FRET signal (15 nM).

The diffusion-enhanced FRET-corrected binding curves for these ligand titrations (Figure 4) show that all ligands induced concentration-dependent and saturable SRC3 recruitment profiles. The EC_{50} values for coactivator recruitment (ligand potency) were 16.2 ± 1.2, 17.2 ± 0.9, 21.8 ± 1.7, and ~151 ± 9 nM for T_3, TRIAC, T_4, and rT_3, respectively (Figure 4 and table). The magnitude of the maximum signal from rT_3, however, was only 40% of that induced by the other three ligands. Because SRC3 binds more weakly to the rT_3−TR complex (Figure 3B), the concentration of SRC3 used in this assay (125 nM) is sufficient to saturate only 40% of this complex.

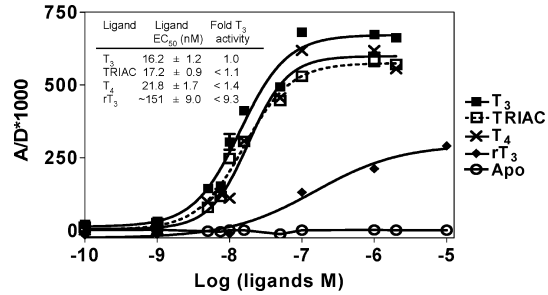

FIGURE 4: Measurement of ligand potency for recruitment of SRC3 to TRE-bound TR·RXR heterodimers (ligand titration). Increasing amounts of different TR ligands were tested for their ability to recruit a submaximal concentration of fluorescein-labeled SRC3 (125 nM) to a fixed amount of TRE-bound TR·RXR (15 nM). tr-FRET values obtained in the presence of each ligand were subtracted from the respective diffusion-enhanced control FRET values and plotted against the log of the ligand concentration. Apo represents the pattern of SRC3 binding to the vehicle-treated TR·RXR heterodimer (unliganded). Each point in the binding curves represents the mean ± standard deviation of six measurements from three different experiments performed in replicate. Data were analyzed as described in the legend of Figure 3B, and the ligand concentration to induce 50% of the maximal SRC3 recruitment was determined and is listed in the table as the mean EC_{50} ± the standard deviation of three independent experiments. Fold T_3 activity was calculated as described in the previous experiment. The Z' factor for T_3-, TRIAC-, T_4-, and rT_3-induced SRC3 recruitment was in the range of 0.76−0.82.

Determination of the Binding Affinity of NCoR for Unliganded TR and Effects of Ligands: Corepressor Titration Assays. To examine NCoR binding to TR, we used an mNCoR NRID fragment (residues 2057−2453) that contains three cysteine residues, all of which are located some distance from the critical CoRNR boxes required for interaction with the TR. In gel shift assays with the DR+4 TRE, this NCoR NRID exhibited good binding activity for the TR·RXR heterodimers, whether fluorescein-labeled or not (data not shown). Fluorescein-labeled NCoR exhibited saturable binding to unliganded TRE-bound TR·RXR (apo), with a measured EC_{50} of 6.9 ± 0.4 nM (Figure 5; curves in panel B are after correction for diffusion-enhanced FRET). NCoR binding to TR complexes with the high-potency agonists, T_3, TRIAC, and T_4, was much more limited and of lower affinity, yet there still appeared to be substantial interaction with the TR−rT_3 complex. These baseline levels of binding with T_3, TRIAC, or T_4 were not reduced when NCoR dissociation was monitored from TR treated with these ligands at 10 or 100 μM. Only at 100 μM, however, did the ligand rT_3 reach a level of NCoR dissociation similar to that observed with T_3, TRIAC, or T_4 at 3 μM (data not shown).

We were curious about the fluorescence activity that remained associated with the TR·RXR heterodimer when saturated with the agonist ligands T_3, TRIAC, and T_4. These background binding signals are clearly above that which can be attributed to diffusion-enhanced tr-FRET (control curve in Figure 5A, which is subtracted from the data in Figure 5B). This NCoR binding does not appear to be due to a small fraction of TR that is unliganded, because it was not significantly reduced in assays performed with a higher concentration of ligands (10 or 100 μM). Thus, we wondered whether it might represent some weak residual binding of NCoR for TR−agonist complexes.

Because the binding surfaces of coactivators and corepressor on NRs are known to partially overlap (*29, 30*), we

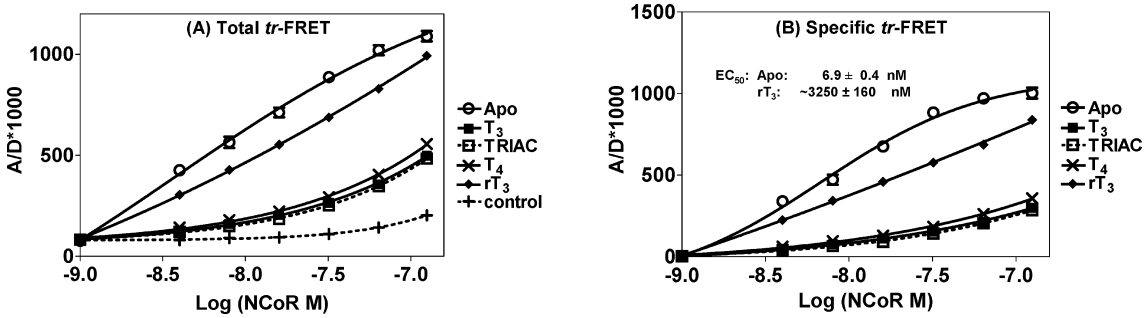

FIGURE 5: Ligand-specific affinity of NCoR for TRE-bound TR·RXR heterodimers (corepressor titration). (A) Serially diluted fluorescein-labeled NCoR was incubated with a fixed amount of DNA-bound TR·RXR (15 nM) in the presence and absence (apo) of the indicated TR ligands (3 μM each), and the resulting tr-FRET signal was measured as described in Experimental Procedures. (B) Binding curves represent results in panel A after correction for diffusion-enhanced tr-FRET. The EC_{50} ± standard deviation of recruitment of NCoR to unliganded TR·RXR from three experiments is shown. In this assay, NCoR recruitment for unliganded TR (apo) had a Z' factor of 0.74.

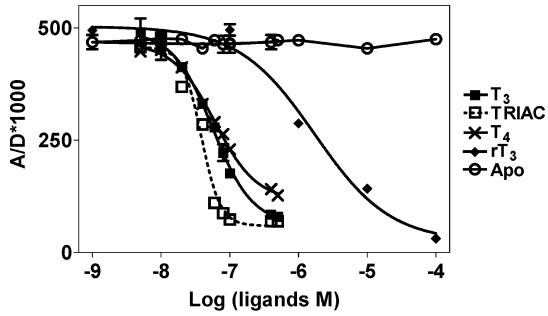

Ligand	Ligand IC_{50} (nM)	Fold T_3 activity
T_3	56.1 ± 3.2	1.0
TRIAC	38.6 ± 2.8	> 1.5
T_4	60.5 ± 4.4	< 1.1
rT_3	1720 ± 52.0	< 31

FIGURE 6: Measurement of ligand potency for dissociation of NCoR from TRE-bound TR·RXR heterodimers (ligand titration). A submaximal concentration of fluorescein-labeled NCoR (24 nM) was incubated with a fixed amount of TR·RXR (15 nM) bound to a TRE in the presence and absence (apo) of indicated concentrations of different TR ligands. The tr-FRET values corrected for diffusion-enhanced tr-FRET values for each of the ligands are shown. Three sets of experiments in replicate were performed, and each point in the curves represents the mean ± standard deviation of six measurements. These data were analyzed by nonlinear regression with an equation for a sigmoidal dose response (variable slope) in GraphPad Prism, and the concentrations of each of the TR ligands to effect 50% dissociation (IC_{50s}) of maximal NCoR binding were obtained and are listed in the table as mean IC_{50} values ± the standard deviation of three different experiments. Fold T_3 activity was calculated as the ratio of respective ligand value IC_{50} to that of T_3. NCoR remained maximally bound to the corresponding unliganded (solvent-treated) TR·RXR sample wells (apo). The Z' factor for each ligand-induced NCoR disociation was measured to be 0.73−0.85.

thought that any residual but specific NCoR binding to agonist-liganded TR·RXR could be disrupted by inclusion of an excess of unlabeled SRC3 in the assay mixture. There were, however, no differences in the level of binding when NCoR interaction assays were carried out both with and without a saturating concentration of unlabeled SRC3 protein (10 μM) in the presence of 100 μM T_3, TRIAC, or T_4 (data not shown). Thus, the residual interaction of NCoR with the agonist-liganded TR is likely due to nonspecific binding.

Determination of Ligand Potency for Dissociation of the TR−NCoR Complex: Ligand Titration. To determine potencies of different TR ligands in the NCoR dissociation assay, we chose a concentration of NCoR (24 nM, determined from the previous experiment) that gave good specific but minimal background tr-FRET signals with 15 nM TRE−TR·RXR complex. All of the ligands, including rT_3, effected a concentration-dependent dissociation of NCoR from the receptor heterodimers, with IC_{50} values of 56.1 ± 3.2, 38.6 ± 2.8, 60.5 ± 4.4, and 1720 ± 52 nM for T_3, TRIAC, T_4, and rT_3, respectively (Figure 6). As we found with ligand titration in the coactivator recruitment assays (Figure 4), the potencies for T_3, TRIAC, and T_4 obtained in this assay were not dramatically different (Figure 6 and table), although TRIAC was consistently more potent than T_3 (1.5-fold) in this corepressor dissociation assay. Thus, the order of TR ligand potency in terms of NCoR displacement is as follows: TRIAC > T_3 ∼ T_4 ≫ rT_3.

As we saw in the SRC3 recruitment assay, rT_3 behaves as an agonist in effecting dissociation of NCoR from TR·RXR, but its low potency (Figure 6) provides an explanation for the substantial affinity of NCoR for the TRE−TR·RXR−rT_3 complex (Figure 5B). The concentration of rT_3 used in the NCoR titration (3 μM) is sufficient to dissociate only 65% of TR-bound NCoR, so unliganded TR in this assay is still available for NCoR binding.

Stability of TR−T_4 and TR−T_3 Complexes: Ligand Dissociation Assays. By radiometric assays, T_4 binds to TR with a 20−30-fold lower affinity than T_3 (*5*–*8*), yet T_4 had activity profiles that are only ∼1.5-fold lower in potency compared to those of T_3 in both of our coregulator interaction assays. Ligand affinity is usually determined by equilibration of a radiolabeled hormone with the receptor protein of interest, in the absence of other interacting protein or DNA partners. The coregulator interaction assays reported here, however, monitor recruitment of SRC3 to or dissociation of NCoR from TR that is heterodimerized with RXR and bound to a TRE.

Previously, we demonstrated that T_4 dissociates more rapidly from TR than T_3, and we suggested that T_4 forms a less stable complex with TR than T_3 does (*6*). We then considered whether the additional components in our more complete assay format (RXR, DR+4 TRE, or SRC3) might have a stabilizing effect on the interaction of T_4 with the TR. Therefore, we examined the kinetic stability of T_4−TR and T_3−TR complexes alone (TR), or as complexes with the other components, TR·RXR, TRE−TR·RXR, or TRE−TR·RXR−SRC3 in ligand dissociation assays. In this assay, a preformed [^{125}I]T_4− or [^{125}I]T_3−TR complex is challenged

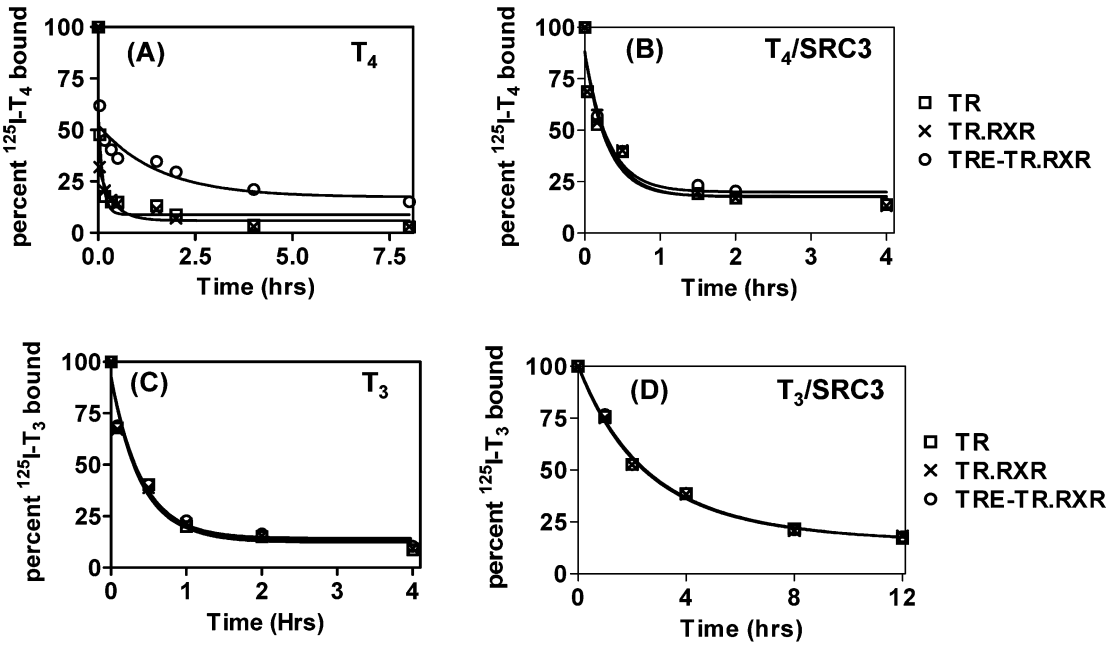

	T_4 $t_{1/2}$		T_3 $t_{1/2}$	
	- SRC3 (mins)	+ SRC3 (mins)	-SRC3 (mins)	+ SRC3 (mins)
TR	1.8 ± 0.09	11.8 ± 1.2	13.4 ± 1.1	132 ± 7.2
TR.RXR	1.3 ± 0.09	13.8 ± 0.6	13.6 ± 0.9	126 ± 5.4
TRE-TR.RXR	5.3 ± 0.30	15.6 ± 0.6	14.0 ± 1.2	126 ± 6.0

FIGURE 7: Ligand dissociation assays. The TR alone or in a complex with RXR or RXR with DR+4 TRE (3.0 nM each) was incubated with 25 nM [^{125}I]T_4 (A) or [^{125}I]T_3 (C) in the absence (total binding) and in the presence of the respective unlabeled hormone at 2.5 μM (nonspecific binding) until the reaction reached equilibrium (12 h at 4 °C). Experiments in panels B and D are similar to those in panels A and C, respectively, but included a saturating concentration of the unlabeled SRC3 NRID fragment (100 nM). Aliquots (50 μL) from the reactions set for total binding were applied to a Sephadex G-25 column (2 mL) before and at the indicated times, after the addition of corresponding unlabeled hormones (2 μM), and the hormone-bound fraction was collected and counted in a γ-counter. The level of nonspecific binding was determined similarly by column fractionation and subtracted from the total level of binding of corresponding experiment to obtain the specific binding. The specific binding from the fraction collected before the addition of unlabeled hormone was set to 100%. Dissociation curves were generated by plotting the percent bound radioactivity vs time. Data were analyzed by nonlinear regression with an equation for three-phase exponential decay. The time taken for 50% dissociation ($t_{1/2}$) is measured from the curve. Each point in the dissociation curves represents the mean ± standard deviation of three independent experiments, and the respective $t_{1/2}$ values are provided in the accompanying table.

with an ~100-fold excess of unlabeled hormone, and the time course of radiolabled hormone dissociation is measured (*6*). A rapid dissociation rate is indicative of a less stable hormone−receptor complex.

Dissociation of T_4 from TR and TR·RXR at 25 °C is very rapid (Figure 7A), having overall half-lives of only 1.3−1.8 min (Figure 7 and table); notably, however, DNA binding markedly slows T_4 dissociation so that in the context of the TRE−TR·RXR complex, T_4 dissociation half-life increases 5.3 min, which is more comparable to the dissociation rate of T_3 [13−14 min in all three receptor contexts (Figure 7C)]. As in our earlier study (*6*), dissociation of both T_4 and T_3 is not a single-exponential process; nevertheless, the effect of TRE is clearly evident both in slowing the overall dissociation rate of T_4 and in reducing the magnitude of the initial, more rapid dissociation phase, whereas the T_3 dissociation profile is unaffected by the inclusion of the TRE.

In the estrogen receptor, we have shown that the binding of coactivators can markedly reduce the rate of dissociation of the agonist−ligand complex (*31*). Here, we find that addition of SRC3 slows dissociation of T_4 from TR and TR·RXR, but less so for the TRE−TR·RXR complex (Figure 7B), resulting in comparable half-lives in all three complexes ($t_{1/2}$ = 12−16 min). These SRC3-induced half-lives of the T_4 complexes are equivalent to the T_3 dissociation times, in all three complexes, without SRC3. Addition of SRC3 to the T_3 complexes, however, provides additional kinetic stabilization, giving them half-lives of ca. 130 min (Figure 7D), which are ca. 8 times greater than those of the T_4−TR complexes in the presence of SRC3 (Figure 7B). In the presence of SRC3, all T_3 and T_4 dissociation profiles are the more cleanly single-exponential type (as analyzed by the equation for a one-phase exponential decay from GraphPad Prism).

Our results indicate that when TR is bound to a DR+4 TRE as a heterodimer with RXR, the T_4−TR interaction is stabilized compared to the interaction of T_4 with TR alone. This effect could be one of the contributing factors for the enhanced T_4 activity in our assays. Nevertheless, once SRC3 is recruited to the liganded TR, TR·RXR, or TRE-bound TR·RXR heterodimer, the T_3−TR interactions are stabilized much more than the T_4−TR interactions, a factor that might account for the higher potency of T_3.

Evaluation of the Synthetic TR Ligands, GC-1 and NH-3, in the Dual Corepressor/Coactivator Interaction Assay. There has been interest in developing agonist compounds

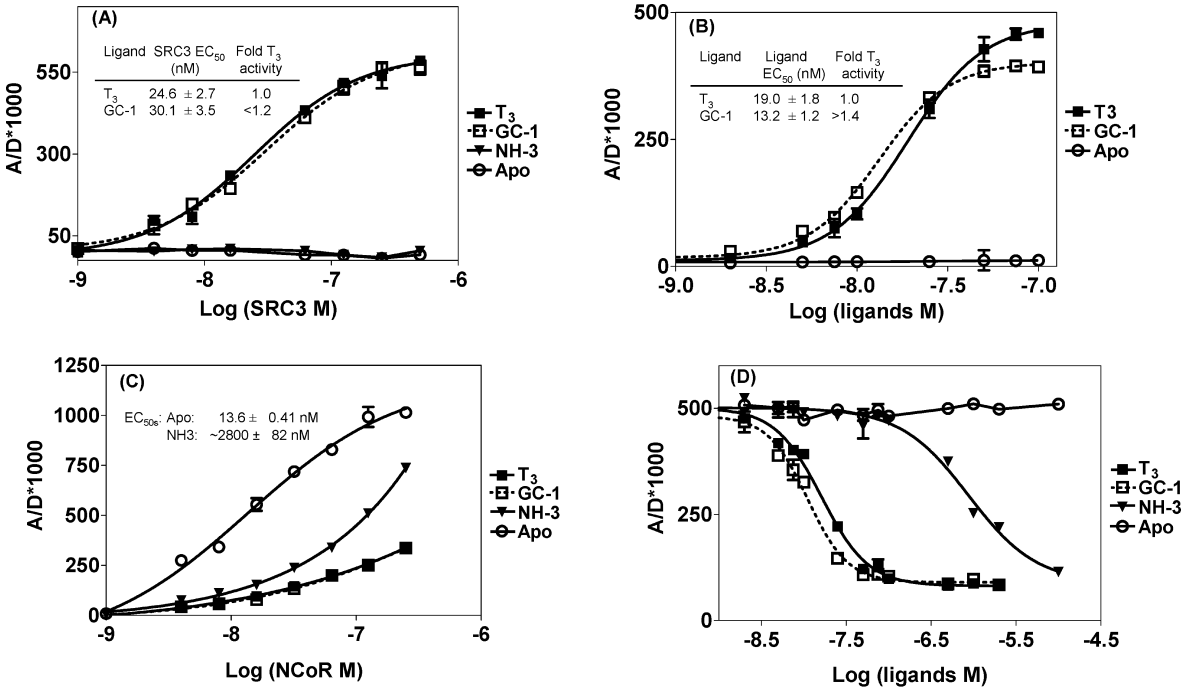

Ligand	Ligand IC_{50} (nM)	Fold T_3 activity
T_3	16.2 ± 1.8	1.0
GC-1	11.1 ± 1.1	> 1.5
NH-3	874 ± 23	< 54

FIGURE 8: Evaluations of GC-1 and NH-3 in the dual coregulator interaction assays. (A) T_3, GC-1, and NH-3 specified affinity of SRC3 for the TRE-bound TR·RXR heterodimer. Serially diluted fluorescein-labeled SRC3 was incubated with DNA-bound TR·RXR (15 nM) in the absence (apo) and presence of T_3, GC-1, and NH-3 (3 μM), and the resulting tr-FRET values were measured. Binding curves after correction for diffusion-enhanced control values are shown. (B) Determination of the potency of T_3 and GC-1 in recruiting SRC3. Different dilutions of T_3 or GC-1 were incubated with TRE-bound TR·RXR (15 nM) and SRC3 (125 nM), and the resulting level of tr-FRET was measured. The specific tr-FRET values are shown. (C) NCoR binding in the presence of T_3, GC-1, and NH-3. TRE-bound TR·RXR was incubated with increasing amounts of fluorescein-labeled NCoR in the absence (apo) and presence of T_3, GC-1, and NH-3 (3 μM), and resulting binding curves after correction for diffusion-enhanced FRET control are shown. (D) Determination of the ligand potency of T_3, GC-1, and NH-3 in the NCoR dissociation assay. The TRE-bound TR·RXR heterodimer was incubated with fluorescein-labeled NCoR (24 nM) in the presence of the indicated levels of T_3, GC-1, and NH-3. The specific tr-FRET values are shown. Data from Figure 7A−D were analyzed by nonlinear regression with an equation for sigmoidal dose response (variable slope) in GraphPad Prism, and the respective EC_{50} and IC_{50} values listed in the corresponding tables represent the means ± standard deviation of three different experiments performed in replicates. The Z' factor for all four formats described here was determined to be in the range of 0.72−0.84.

that elicit desirable tissue-selective but not unwanted actions of thyroid hormone and also antagonists that block TH action for treatment of thyroid excess state. The ligand GC-1 (Figure 1) displays selectivity both in its tissue uptake properties and for the β versus α isoforms of the TR; it promotes weight loss and lowers cholesterol without eliciting deleterious cardiac effects and is being evaluated as a potential pharmaceutical (*17, 32*). The TR antagonist NH-3 (Figure 1) can block tadpole metamorphosis (*33*).

We measured potencies and coregulator binding characteristics of these novel TR ligands in our four assay formats, together with T_3 as a reference. In SRC3 titrations with TRE-bound TR·RXR incubated with these three ligands (each at 3 μM), SRC3 binding to T_3– and GC-1–TR complexes showed saturation curves with EC_{50} values of 24.6 ± 2.7 and 30.1 ± 3.5 nM, respectively (Figure 8A). By contrast, SRC3 shows no binding affinity for TR liganded with the antagonist NH-3, consistent with its antagonistic activity in vivo (*18*). Increasing the NH-3 concentration to 25 or 100 μM had no effect on recruitment of SRC3 to TR (data not shown). In ligand titration assays, EC_{50} values for T_3 and GC-1 were 19.0 ± 1.8 and 13.2 ± 1.2 nM, respectively, indicating that GC-1 is slightly more potent that T_3 in recruiting SRC3 to the DNA-bound TR·RXR heterodimer (Figure 8B). These findings are consistent with the similar affinities of T_3 and GC-1 for TRβ and their nearly identical efficacies in mammalian cell transactivation assays (*17*).

In TR−corepressor dissociation assays (Figure 8C), NCoR exhibited, as before, essentially no affinity for TRE-bound TR·RXR liganded with agonists GC-1 and T_3, but saturable binding to unliganded TR. NCoR did exhibit binding to the TRE-bound TR·RXR heterodimers in the presence of 3 μM NH-3, although it did so with very low potency (EC_{50} value of 2800 ± 82 nM). We believe this low-affinity interaction reflects the fact that the concentration of NH-3 used in this assay (3 μM) is not sufficient to fully saturate TR, leaving some unliganded TR with which NCoR can interact. Consistently, interaction of NCoR with TR performed with different NH-3 concentrations revealed that maximal inhibition of NCoR binding was observed only at 25 μM NH-3 (data not shown). In ligand titration assays, both GC-1 and NH-3 effected dissociation of NCoR from apo-TR·RXR

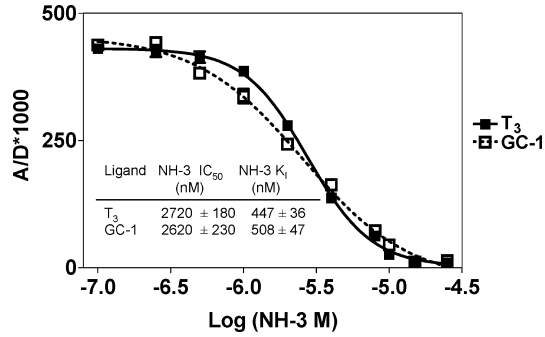

FIGURE 9: NH-3 blocks T_3- and GC-1-induced SRC3 recruitment to the TRE-bound TR·RXR heterodimer. Increasing amounts of NH-3 were tested for their ability to block recruitment of fluorescein-labeled SRC3 to TR·RXR by a submaximal dose of T_3 or GC-1 (30 nM). NH-3 displacement curves that were corrected for diffusion-enhanced FRET were analyzed by nonlinear regression with an equation for sigmoidal dose response (variable slope) in GraphPad Prism, and the concentration of NH-3 to displace 50% of T_3- or GC-1-induced SRC3 recruitment was determined (Figure 9 table). These IC_{50} values and the EC_{50} values from Figure 8A (which approximate the apparent affinity of SRC3 for TRE-bound TR·RXR in the presence of T_3 and GC-1) were used with the Cheng−Prusoff equation to estimate the relative affinity of NH-3 for displacement of SRC3 recruited to TR by T_3 or GC-1. The Cheng−Prusoff equation is $K_I = IC_{50}/(1 + T_0/K_D^*)$, where IC_{50} is the concentration of NH-3 giving 50% inhibition of T_3- or GC-1-induced SRC3 recruitment (IC_{50} from Figure 9 table), K_I is the dissociation constant of NH-3 that is to be determined, T_0 is the concentration of SRC3 used in the experiment (125 nM), and K_D^* is the EC_{50} value obtained from the SRC3 saturation binding curves in the presence of T_3 and GC-1, at 24.6 and 30.1 nM, respectively (Figure 8A and table). The determined apparent K_I values are listed in the table. Three independent experiments in replicate were performed, and the NH-3 IC_{50} values in the Figure 9 table represent the mean ± standard deviation from three different experiments.

(Figure 8D), with GC-1 being slightly more potent than T_3. NH-3 also disrupted TR-NCoR binding, although with a much lower potency. The IC_{50} values were 16.2 ± 1.8, 11.1 ± 1.1, and 874 ± 23 nM for T_3, GC-1, and NH-3, respectively, and are consistent with the binding affinities of these ligands (*17, 18*).

NH-3 Blocks T_3- and GC-1-Mediated SRC3 Recruitment. To determine whether the antagonist NH-3 could reverse the recruitment of SRC3 to TRE-bound TR·RXR induced by T_3 or GC-1, we titrated increasing concentrations of NH-3 into an assay in which SRC3 had been recruited to TR with 30 nM T_3 or GC-1. Good competition curves were seen in both cases (Figure 9), giving IC_{50} values of 2720 ± 180 and 2620 ± 230 nM, respectively. The apparent K_i values, obtained by correcting the IC_{50} values for the concentrations of T_3 or GC-1 used in this experiment (30 nM), were 447 ± 36 and 508 ± 47 nM, for NH-3 in competition with T_3 and GC-1, respectively, values that are consistent with the K_i values from inhibition curves of NH-3 suppression of T_3- and GC-1-induced transactivation in reporter gene assays (*18*).

DISCUSSION

Determinants of Nuclear Receptor Agonist Ligand Potency: Ligand−Receptor Interaction and Coregulator−Receptor Interaction Measured in Vitro in a Biologically Relevant Context. Elucidation of the molecular components involved in NR regulation of target gene transcription suggests that the potency of a NR agonist in a cellular context will reflect both its affinity for binding to the receptor and the affinity with which coactivator proteins are able to interact with the resulting agonist−NR complex. It is straightforward to measure ligand−receptor binding affinities directly by titrations in two-component (ligand and receptor) systems, assayed by radiometric or fluorometric methods, or to estimate them by ligand titrations in coactivator recruitment assays. Neither of these methods, however, reveals the affinity with which coregulators bind to different ligand−receptor complexes. The favorable attributes of our tr-FRET assay system enabled us to measure these protein−protein binding affinities directly.

A Convenient and Quantifiable tr-FRET Assay for Ligand Regulation of TR−Coregulator Interactions. The different protein components used in our tr-FRET assays of the TR and THs have been characterized well in terms of mediating protein−protein interactions with NRs (NCoR and SRC3 NRIDs) and for their near-normal ligand binding, DNA binding, and in vitro transcriptional regulatory properties (TR and RXR) (*21–23, 34*). We selected a natural DR+4 sequence from the rat myosin heavy chain promoter as the DNA component because, unlike palindromic or inverted palindromic sequences, both liganded and unliganded TR·RXR heterodimers bind DR+4 TRE with high affinity, ensuring that the changes we observe in tr-FRET are due to changes in ligand-specific coregulator binding and not alterations in DNA binding (*4, 35*). To the best of our knowledge, this is the first report assessing quantitatively the affinity of both a coactivator and a corepressor for a response element-bound NR ligand complex, and thus, it represents a significant step toward mimicry of the cellular context in which a NR normally works to regulate transcription.

The terbium donor fluorophore used in these tr-FRET assays provides some particularly favorable properties: a pronounced Stokes shift, a large R_0 value, and a long fluorescence lifetime (1 ms). The last of these enables pulsed excitation and gated emission measurement, which greatly minimizes signals due to background or direct excitation of the acceptor fluorophore (*36–39*), and makes feasible titration experiments with acceptor fluorophore (fluorescein)-labeled coregulators; such titrations are more difficult to do with conventional FRET assays. Thus, with tr-FRET we can measure two distinct parameters: (i) the affinity of coregulators for the receptor (either apo-TR or the various TR−ligand complexes) measured in a coregulator titration experiment and (ii) the potency of ligands in regulating interaction of the receptor with the coactivator or corepressor measured in a ligand titration experiment.

Potencies and Efficacies of Thyroid Hormones. The potency and agonistic and antagonistic activities of THs are usually determined by standard reporter gene assays using mammalian cell lines in culture (*7, 8, 17, 18, 40*). A comprehensive evaluation of how both natural and synthetic THs affect coactivator and corepressor interactions in terms of their binding efficiency and affinity for the TRE-bound TR·RXR heterodimer in vitro is typically not undertaken, however, because suitable, quantitative assay systems are not available. In addition, it is not even known whether the potency of a given TR ligand in mediating the distinct process of corepressor dissociation versus coactivator as-

sociation is the same or different, or to what extent the potency of a TH agonist depends on its affinity for the TR versus the affinity with which coactivators bind to the ligand−receptor complex it forms with the TR.

The rank order of potencies we obtain for the THs by the ligand titration coactivator recruitment assay ($T_3 \sim$ TRIAC $\sim T_4 \gg rT_3$) is very similar to the rank order of relative affinities of SRC3 for the respective ligand−TR complexes, with the first three (T_3, TRIAC, and T_4) being the same within a factor of 1.5 and the fourth (rT_3) being 10−20-fold lower. The concordance between the affinity of a ligand for its receptor and the affinity of a ligand−receptor complex for a coactivator, however, is not necessarily expected, and it is worth considering what these results mean for a poor TR ligand, such as rT_3. The low potency of this ligand appears to be caused by two factors: (i) its low affinity for binding to TR and (ii) the weak affinity that SRC3 has for the resulting rT_3−TR complex. Thus, while an increasing rT_3 concentration could compensate for the low affinity that rT_3 has for the TR, no increase in ligand concentration could compensate for its second "deficiency", the fact that the complex that rT_3 makes with the TR has itself a lower affinity for SRC3. Our findings with rT_3 could have broad pharmacological implications: They suggest that while high concentrations of a low-affinity ligand may saturate a receptor, the biological output from this complex might not be equivalent to that of a receptor complex with a high-affinity ligand, because it would be unable to interact effectively with the downstream signaling components required to mediate further biological effects.

It is notable that the crystal structure of TRβ complexed with T_4 shows that the receptor can undergo subtle structural alterations relative to the crystal structure of the TRβ−T_3 complex to accommodate the bulky 5′-iodine group of T_4 (*6*). Despite these changes, the TR−T_4 complex maintains its affinity for SRC3. While there is no crystal structure for the TR−rT_3 complex, the reduced affinity of SRC3 for this complex suggests that its conformation is significantly different from the conformations of those TR complexes with T_3 and T_4.

The order of ligand potency in terms of corepressor dissociation is as follows: TRIAC $\geq T_3 \sim T_4 > rT_3$ [with rT_3 being some 30-fold weaker than the other three (Figure 6 table), which is similar to that found in the coactivator recruitment assays]. Interestingly, however, we repeatedly found TRIAC to be the most potent TR ligand (1.5-fold more potent than T_3) in the ligand titrations of NCoR dissociation, hinting at the possibility that ligands like TRIAC might be more effective in transcriptional derepression than transcriptional activation functions. While the ligand rT_3 was the least potent, it still promoted both NCoR dissociation and SRC3 recruitment, which are attributes of a TH agonist.

tr-FRET and other types of fluorescence-based assays have been used to study the interaction of coactivators with other NRs (*39, 41–43*), and while they have provided some information about the binding affinity and the efficacy of various ligands, they have been conducted in less "intact" systems (i.e., lacking hormone response elements and using NR ligand-binding domains and short peptide sequences from coregulators). The studies of androgen receptors also revealed the effect of mutations on the agonist−antagonist balance of various ligands (*38*). The role of coactivator binding affinity as a codeterminant of ligand potency, however, has thus far not been studied in a coherent fashion. Other workers have used fingerprinting methods to characterize the interaction of NR with panels of peptides from both known coregulators or phage display-derived methods (*44, 45*). While these approaches provide a broader view of NR−coregulator interactions, they do not provide quantitative affinities.

Reciprocal Interactions of DNA and Coactivator on TR−Ligand Complex Stability and Conformation. We were curious that in our assays T_4 appeared to be comparable to T_3 and TRIAC in terms of potency in SRC3 recruitment and NCoR dissociation and in terms of the binding affinity of SRC3 for the three TR−ligand complexes. In other assays, however, T_4 has been found to have a lower potency than T_3 and TRIAC (*5, 7, 8*). Because various NRs, including estrogen and glucocorticoid receptors and TRs, undergo specific conformational changes upon binding to different response elements, resulting in selective recruitment of coactivator and corepressor proteins and ultimately altering the transcriptional response to a particular ligand (*25, 35, 46–49*), we wondered whether the higher relative potency of T_4 in our hands might be due to a selective stabilizing effect of the heterodimer partner RXR, the TRE, or the coactivator components on the TR−T_4 complex relative to the TR−T_3 complex.

From ligand dissociation rate measurements, we found that the rapid dissociation of T_4 from TR was moderated to some extent by the addition of TRE, but T_3 dissociation was unaffected. Given the fact that circulating level of free T_4 is ~7 times higher than that of T_3 in humans (*50*), this suggests that T_4 might be more effective in vivo, despite its lower affinity for TR. The rate of dissociation of T_3 from the TR, TR·RXR, or TRE-bound TR·RXR, however, is still slower than that of T_4. Furthermore, like the effect that SRC1 has on slowing the dissociation rate of estrogen agonists in estrogen receptor α (*31*), we found that the addition of SRC3 afforded kinetic stabilization of the TR−ligand complexes, with stabilization, in fact, being greater for T_3 and for T_4 (from 1.3−5.3 to 11.8−15.6 min for T_4 and from 13.4−14.0 to 126−132 min for T_3), with a similar degree in shift of the half-life between T_4 and T_3 with the addition of SRC3 (3−10-fold shift in T_4 vs ~10-fold shift in T_3). This indicates that the coactivator stabilization process is ligand structure-dependent and is another factor contributing to overall ligand potency. Thus, we ascribe the more comparable potency of T_4 relative to T_3 and TRIAC we observe to a potency-leveling effect that results from the relatively high concentration of TR (15 nM) required to obtain adequate FRET signal levels in our assays.

Characterization of the Bioactivity of the Novel TR ligands, CG-1 and NH-3. Our results with GC-1, a synthetic T_3 agonist, and NH-3, a synthetic T_3 antagonist, are in good agreement with the TRβ binding affinities, potencies, and efficacies of these compounds measured in cell-based assays. GC-1 has approximately the same affinity as T_3 for TRβ and profiles as a potent agonist (*17*). Likewise, NH-3 lacks agonist activity and completely blocks T_3-driven gene activity in transfection assays, yet in mammalian two-hybrid assays, it dissociates corepressors from TR, albeit weakly (*18*). We too found that NH-3 failed to recruit SRC3 to the TR and displayed a relatively low potency for corepressor dissocia-

tion; we were able to quantify the relative NCoR dissociation potency by NH-3 to be ca. 50 times less than that of GC-1 and T_3, which is similar to the NH-3 to T_3 potency ratio of 30 obtained in cell-based assays (*18*).

CONCLUSION

We have described a dual, in vitro tr-FRET-based assay through which the interaction of DNA-bound TR·RXR heterodimers with a coactivator (SRC3) and a corepressor (NCoR), both bona fide coregulators for TRs, can be assessed in response to the binding of various thyroid hormones and their analogues. This assay is convenient (mix and measure format), miniaturizable (15−20 μL), readily quantifiable, and reproducible (Z' factor in the range of 0.72−0.84) (*26*). We provide several lines of evidence showing that these interactions are specific and that the potency and efficacy values we measure in this assay are predictive of the inherent potencies and the agonistic or antagonistic nature of various TR ligands. We can also clearly distinguish the corepressor dissociation and coactivator recruitment characteristics of TR agonists versus TR antagonists. Furthermore, we can determine the affinity with which SRC3 interacts with TR complexes with different agonist ligands, an interaction that can modulate overall ligand potency in a cellular context but has thus far been difficult to quantify. The assay system developed here can be easily extended to determine how other TREs, such as palindromic and inverted palindromic response elements, influence TR ligand potencies and how they compare to that obtained with DR+4 TRE. Thus, our results provide new insight into the molecular interactions that underlie agonist ligand potency and the nature of antagonism of various TR ligands. It is notable, as well, that the type of tr-FRET assay we employ can be modified using two acceptor fluorophores so that coactivator recruitment and corepressor dissociation can be assessed simultaneously in a single assay, as we have done with TRE-bound TR·RXR and SRC3 and NCoR (M. Jeyakumar and J. A. Katzenellenbogen, unpublished observations) and as recently reported in a different system (*51*). It is likely that assays of this type, with yet further refinement in components and context, will play an increasingly important role in identifying and characterizing novel ligands for members of the NR family.

ACKNOWLEDGMENT

We thank Dr. Milan K. Bagchi for providing the constructs for TR, RXR, and NCoR and Dr. Varsha S. Likhite, Jillian R. Gunther, Kathryn E. Carlson, and Dr. Sung Hoon Kim for helpful discussions.

REFERENCES

1. Lonard, D. M., and O'Malley, B. W. (2005) Expanding functional diversity of the coactivators. *Trends Biochem. Sci. 30*, 126–132.
2. Privalsky, M. L. (2004) The role of corepressors in transcriptional regulation by nuclear hormone receptors. *Annu. Rev. Physiol. 66*, 315–360.
3. Yen, P. M., Ando, S., Feng, X., Liu, Y., Maruvada, P., and Xia, X. (2006) Thyroid hormone action at the cellular, genomic and target gene levels. *Mol. Cell. Endocrinol. 246*, 121–127.
4. Lazar, M. A. (1993) Thyroid hormone receptors: Multiple forms, multiple possibilities. *Endocr. Rev. 14*, 184–193.
5. Apriletti, J. W., Eberhardt, N. L., Latham, K. R., and Baxter, J. D. (1981) Affinity chromatography of thyroid hormone receptors. Biospecific elution from support matrices, characterization of the partially purified receptor. *J. Biol. Chem. 256*, 12094–12101.
6. Sandler, B., Webb, P., Apriletti, J. W., Huber, B. R., Togashi, M., Cunha Lima, S. T., Juric, S., Nilsson, S., Wagner, R., Fletterick, R. J., and Baxter, J. D. (2004) Thyroxine-thyroid hormone receptor interactions. *J. Biol. Chem. 279*, 55801–55808.
7. Schueler, P. A., Schwartz, H. L., Strait, K. A., Mariash, C. N., and Oppenheimer, J. H. (1990) Binding of 3,5,3′-triiodothyronine (T3) and its analogs to the in vitro translational products of c-erbA protooncogenes: Differences in the affinity of the α- and β-forms for the acetic acid analog and failure of the human testis and kidney α-2 products to bind T3. *Mol. Endocrinol. 4*, 227–234.
8. Weinberger, C., Thompson, C. C., Ong, E. S., Lebo, R., Gruol, D. J., and Evans, R. M. (1986) The c-erb-A gene encodes a thyroid hormone receptor. *Nature 324*, 641–646.
9. Ribeiro, R. C., Apriletti, J. W., Wagner, R. L., West, B. L., Feng, W., Huber, R., Kushner, P. J., Nilsson, S., Scanlan, T., Fletterick, R. J., Schaufele, F., and Baxter, J. D. (1998) Mechanisms of thyroid hormone action: Insights from X-ray crystallographic and functional studies. *Recent Prog. Horm. Res. 53*, 351–392.
10. Ribeiro, R. C., Kushner, P. J., Apriletti, J. W., West, B. L., and Baxter, J. D. (1992) Thyroid hormone alters in vitro DNA binding of monomers and dimers of thyroid hormone receptors. *Mol. Endocrinol. 6*, 1142–1152.
11. Tsai, M. J., and O'Malley, B. W. (1994) Molecular mechanisms of action of steroid/thyroid receptor superfamily members. *Annu. Rev. Biochem. 63*, 451–486.
12. Yen, P. M., Darling, D. S., Carter, R. L., Forgione, M., Umeda, P. K., and Chin, W. W. (1992) Triiodothyronine (T3) decreases binding to DNA by T3-receptor homodimers but not receptor-auxiliary protein heterodimers. *J. Biol. Chem. 267*, 3565–3568.
13. Jung, S. Y., Malovannaya, A., Wei, J., O'Malley, B. W., and Qin, J. (2005) Proteomic analysis of steady-state nuclear hormone receptor coactivator complexes. *Mol. Endocrinol. 19*, 2451–2465.
14. Moore, J. M., and Guy, R. K. (2005) Coregulator interactions with the thyroid hormone receptor. *Mol. Cell. Proteomics 4*, 475–482.
15. Chen, J. D., and Evans, R. M. (1995) A transcriptional co-repressor that interacts with nuclear hormone receptors. *Nature 377*, 454–457.
16. Horlein, A. J., Naar, A. M., Heinzel, T., Torchia, J., Gloss, B., Kurokawa, R., Ryan, A., Kamei, Y., Soderstrom, M., Glass, C. K., and Rosenfeld, M. G. (1995) Ligand-independent repression by the thyroid hormone receptor mediated by a nuclear receptor co-repressor. *Nature 377*, 397–404.
17. Chiellini, G., Apriletti, J. W., Yoshihara, H. A., Baxter, J. D., Ribeiro, R. C., and Scanlan, T. S. (1998) A high-affinity subtype-selective agonist ligand for the thyroid hormone receptor. *Chem. Biol. 5*, 299–306.
18. Nguyen, N. H., Apriletti, J. W., Cunha Lima, S. T., Webb, P., Baxter, J. D., and Scanlan, T. S. (2002) Rational design and synthesis of a novel thyroid hormone antagonist that blocks coactivator recruitment. *J. Med. Chem. 45*, 3310–3320.
19. Izumo, S., and Mahdavi, V. (1988) Thyroid hormone receptor α isoforms generated by alternative splicing differentially activate myosin HC gene transcription. *Nature 334*, 539–542.
20. Jeyakumar, M., Tanen, M. R., and Bagchi, M. K. (1997) Analysis of the functional role of steroid receptor coactivator-1 in ligand-induced transactivation by thyroid hormone receptor. *Mol. Endocrinol. 11*, 755–767.
21. Tong, G. X., Jeyakumar, M., Tanen, M. R., and Bagchi, M. K. (1996) Transcriptional silencing by unliganded thyroid hormone receptor β requires a soluble corepressor that interacts with the ligand-binding domain of the receptor. *Mol. Cell. Biol. 16*, 1909–1920.
22. Zhang, X., Jeyakumar, M., Petukhov, S., and Bagchi, M. K. (1998) A nuclear receptor corepressor modulates transcriptional activity of antagonist-occupied steroid hormone receptor. *Mol. Endocrinol. 12*, 513–524.
23. Kim, S. H., Tamrazi, A., Carlson, K. E., and Katzenellenbogen, J. A. (2005) A proteomic microarray approach for exploring ligand-initiated nuclear hormone receptor pharmacology, receptor selectivity, and heterodimer functionality. *Mol. Cell. Proteomics 4*, 267–277.
24. Tamrazi, A., and Katzenellenbogen, J. A. (2003) Site-specific fluorescent labeling of estrogen receptors and structure-activity relationships of ligands in terms of receptor dimer stability. *Methods Enzymol. 364*, 37–53.
25. Likhite, V. S., Stossi, F., Kim, K., Katzenellenbogen, B. S., and Katzenellenbogen, J. A. (2006) Kinase-specific phosphorylation of the estrogen receptor changes receptor interactions with ligand,

deoxyribonucleic acid, and coregulators associated with alterations in estrogen and tamoxifen activity. *Mol. Endocrinol. 20*, 3120–3132.
26. Zhang, J. H., Chung, T. D., and Oldenburg, K. R. (1999) A Simple Statistical Parameter for Use in Evaluation and Validation of High Throughput Screening Assays. *J. Biomol. Screening 4*, 67–73.
27. Cheng, Y., and Prusoff, W. H. (1973) Relationship between the inhibition constant (K1) and the concentration of inhibitor which causes 50% inhibition (I50) of an enzymatic reaction. *Biochem. Pharmacol. 22*, 3099–3108.
28. Takeshita, A., Cardona, G. R., Koibuchi, N., Suen, C. S., and Chin, W. W. (1997) TRAM-1, a novel 160-kDa thyroid hormone receptor activator molecule, exhibits distinct properties from steroid receptor coactivator-1. *J. Biol. Chem. 272*, 27629–27634.
29. Marimuthu, A., Feng, W., Tagami, T., Nguyen, H., Jameson, J. L., Fletterick, R. J., Baxter, J. D., and West, B. L. (2002) TR surfaces and conformations required to bind nuclear receptor corepressor. *Mol. Endocrinol. 16*, 271–286.
30. Nagy, L., Kao, H. Y., Love, J. D., Li, C., Banayo, E., Gooch, J. T., Krishna, V., Chatterjee, K., Evans, R. M., and Schwabe, J. W. (1999) Mechanism of corepressor binding and release from nuclear hormone receptors. *Genes Dev. 13*, 3209–3216.
31. Gee, A. C., Carlson, K. E., Martini, P. G., Katzenellenbogen, B. S., and Katzenellenbogen, J. A. (1999) Coactivator peptides have a differential stabilizing effect on the binding of estrogens and antiestrogens with the estrogen receptor. *Mol. Endocrinol. 13*, 1912–1923.
32. Baxter, J. D., Webb, P., Grover, G., and Scanlan, T. S. (2004) Selective activation of thyroid hormone signaling pathways by GC-1: A new approach to controlling cholesterol and body weight. *Trends Endocrinol. Metab. 15*, 154–157.
33. Lim, W., Nguyen, N. H., Yang, H. Y., Scanlan, T. S., and Furlow, J. D. (2002) A thyroid hormone antagonist that inhibits thyroid hormone action in vivo. *J. Biol. Chem. 277*, 35664–35670.
34. Jeyakumar, M., Liu, X. F., Erdjument-Bromage, H., Tempst, P., and Bagchi, M. K. (2007) Phosphorylation of thyroid hormone receptor-associated nuclear receptor corepressor holocomplex by the DNA-dependent protein kinase enhances its histone deacetylase activity. *J. Biol. Chem. 282*, 9312–9322.
35. Velasco, L. F., Togashi, M., Walfish, P. G., Pessanha, R. P., Moura, F. N., Barra, G. B., Nguyen, P., Rebong, R., Yuan, C., Simeoni, L. A., Ribeiro, R. C., Baxter, J. D., Webb, P., and Neves, F. A. (2007) Thyroid hormone response element organization dictates the composition of active receptor. *J. Biol. Chem. 282*, 12458–12466.
36. Bramlett, K. S., Wu, Y., and Burris, T. P. (2001) Ligands specify coactivator nuclear receptor (NR) box affinity for estrogen receptor subtypes. *Mol. Endocrinol. 15*, 909–922.
37. Gowda, K., Marks, B. D., Zielinski, T. K., and Ozers, M. S. (2006) Development of a coactivator displacement assay for the orphan receptor estrogen-related receptor-γ using time-resolved fluorescence resonance energy transfer. *Anal. Biochem. 357*, 105–115.
38. Ozers, M. S., Marks, B. D., Gowda, K., Kupcho, K. R., Ervin, K. M., De Rosier, T., Qadir, N., Eliason, H. C., Riddle, S. M., and Shekhani, M. S. (2007) The androgen receptor T877A mutant recruits LXXLL and FXXLF peptides differently than wild-type androgen receptor in a time-resolved fluorescence resonance energy transfer assay. *Biochemistry 46*, 683–695.
39. Zhou, G., Cummings, R., Li, Y., Mitra, S., Wilkinson, H. A., Elbrecht, A., Hermes, J. D., Schaeffer, J. M., Smith, R. G., and Moller, D. E. (1998) Nuclear receptors have distinct affinities for coactivators: Characterization by fluorescence resonance energy transfer. *Mol. Endocrinol. 12*, 1594–1604.
40. Thompson, C. C., and Evans, R. M. (1989) Trans-activation by thyroid hormone receptors: Functional parallels with steroid hormone receptors. *Proc. Natl. Acad. Sci. U.S.A. 86*, 3494–3498.
41. Stafslien, D. K., Vedvik, K. L., De Rosier, T., and Ozers, M. S. (2007) Analysis of ligand-dependent recruitment of coactivator peptides to RXRβ in a time-resolved fluorescence resonance energy transfer assay. *Mol. Cell. Endocrinol. 264*, 82–89.
42. Ozers, M. S., Ervin, K. M., Steffen, C. L., Fronczak, J. A., Lebakken, C. S., Carnahan, K. A., Lowery, R. G., and Burke, T. J. (2005) Analysis of ligand-dependent recruitment of coactivator peptides to estrogen receptor using fluorescence polarization. *Mol. Endocrinol. 19*, 25–34.
43. Margeat, E., Poujol, N., Boulahtouf, A., Chen, Y., Muller, J. D., Gratton, E., Cavailles, V., and Royer, C. A. (2001) The human estrogen receptor α dimer binds a single SRC-1 coactivator molecule with an affinity dictated by agonist structure. *J. Mol. Biol. 306*, 433–442.
44. Bramlett, K. S., and Burris, T. P. (2002) Effects of selective estrogen receptor modulators (SERMs) on coactivator nuclear receptor (NR) box binding to estrogen receptors. *Mol. Genet. Metab. 76*, 225–233.
45. Iannone, M. A., Simmons, C. A., Kadwell, S. H., Svoboda, D. L., Vanderwall, D. E., Deng, S. J., Consler, T. G., Shearin, J., Gray, J. G., and Pearce, K. H. (2004) Correlation between in vitro peptide binding profiles and cellular activities for estrogen receptor-modulating compounds. *Mol. Endocrinol. 18*, 1064–1081.
46. Ikeda, M., Wilcox, E. C., and Chin, W. W. (1996) Different DNA elements can modulate the conformation of thyroid hormone receptor heterodimer and its transcriptional activity. *J. Biol. Chem. 271*, 23096–23104.
47. Klinge, C. M., Jernigan, S. C., Mattingly, K. A., Risinger, K. E., and Zhang, J. (2004) Estrogen response element-dependent regulation of transcriptional activation of estrogen receptors α and β by coactivators and corepressors. *J. Mol. Endocrinol. 33*, 387–410.
48. Lefstin, J. A., Thomas, J. R., and Yamamoto, K. R. (1994) Influence of a steroid receptor DNA-binding domain on transcriptional regulatory functions. *Genes Dev. 8*, 2842–2856.
49. Takeshita, A., Yen, P. M., Ikeda, M., Cardona, G. R., Liu, Y., Koibuchi, N., Norwitz, E. R., and Chin, W. W. (1998) Thyroid hormone response elements differentially modulate the interactions of thyroid hormone receptors with two receptor binding domains in the steroid receptor coactivator-1. *J. Biol. Chem. 273*, 21554–21562.
50. Bianco, A. C., Salvatore, D., Gereben, B., Berry, M. J., and Larsen, P. R. (2002) Biochemistry, cellular and molecular biology, and physiological roles of the iodothyronine selenodeiodinases. *Endocr. Rev. 23*, 38–89.
51. Kupcho, K. R., Stafslien, D. K., DeRosier, T., Hallis, T. M., Ozers, M. S., and Vogel, K. W. (2007) Simultaneous monitoring of discrete binding events using dual-acceptor terbium-based LRET. *J. Am. Chem. Soc. 129*, 13372–13373.

BI800393U